Supplementary material to the paper "Current-limiting control strategies in variable capacitance electrostatic energy harvesters"

Alireza Jalaliankhakshour[1], Gianluca Rizzello[2], Antonello Cherubini[1], Marco Fontana[3], and Giacomo Moretti*[1]

[1]Department of Industrial Engineering, University of Trento, Trento, Italy
[2]Department of Systems Engineering, Saarland University, Saarbrücken, Germany
[3]Institute of Mechanical Intelligence, Scuola Superiore Sant'Anna, Pisa, Italy

S1 Experimental setup

A schematic and a photograph of the experimental setup are shown in Fig. S1. The setup comprises:

- A linear motor (DM01-37x120F-HP-R-95 by LinMot) with driver (C1250-MI-XC-1S-000) to position control the DEG sample
- A custom designed clamping mechanism for the DEG
- A high voltage amplifier (HAR42-4 rack with HA3B3-S amplifier module) with integrated voltage monitor, that was used to apply controlled voltage waveforms on the DEG, and measure the apply voltage
- A picoammeter (Keithley 6485) with analog output monitor was connected in series to the DEG on the ground side and was used to measure the current
- A real-time Target Performance Machine, running Matlab Realtime, which was used to closed-loop control the system and acquire all measurements.

The real-time target machine

- Acquires analog inputs corresponding to measurements of the DEG voltage (from the amplifier monitor), current (from the picoammeter analog output port), motor position (through the motor in-built resolver)
- Provides the position command (as an analog output) to the motor driver, according to a pre-defined position trajectory.
- Executes the control logics in real-time based on the measured signals (e.g., by implementing the observer-like filter described in Sect. 2.4, or peak detection algorithms for peak-triggered control) and provides a reference voltage signal (in the form of an analog output) to the amplifier.

*Corresponding author.
E-mail: giacomo.moretti@unitn.it

The DEG was securely held in place using custom 3D-printed PETG clamps, designed specifically to prevent membrane slippage during operation (Fig. S2). The clamp consists of a top and bottom plate, which are tightened together using multiple bolts to ensure uniform pressure distribution along the DEG. At the core of the design is a curved insert with a concave profile, w hich s ignificantly increases the contact area and improves grip. Additionally, the insert features a recessed groove that creates a mechanical interlock with the membrane, physically preventing lateral movement when the DEG is under tension. Guide holes ensure precise alignment of the plates and parallelism during assembly, eliminating shear forces that could otherwise lead to slippage. The use of PETG as the clamp material further enhances friction while avoiding damage to the elastomer.

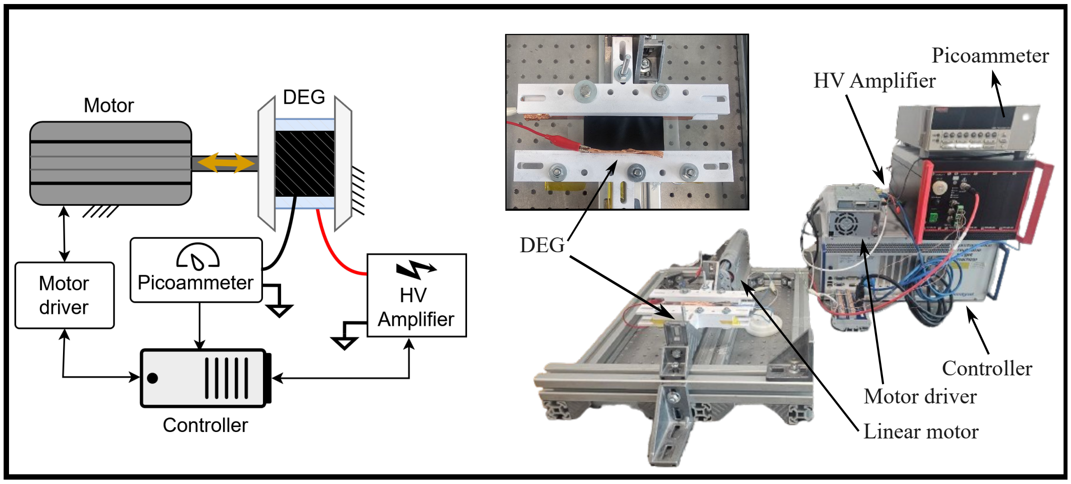

Figure S1: Schematic (left) and picture (right) of the experimental setup.

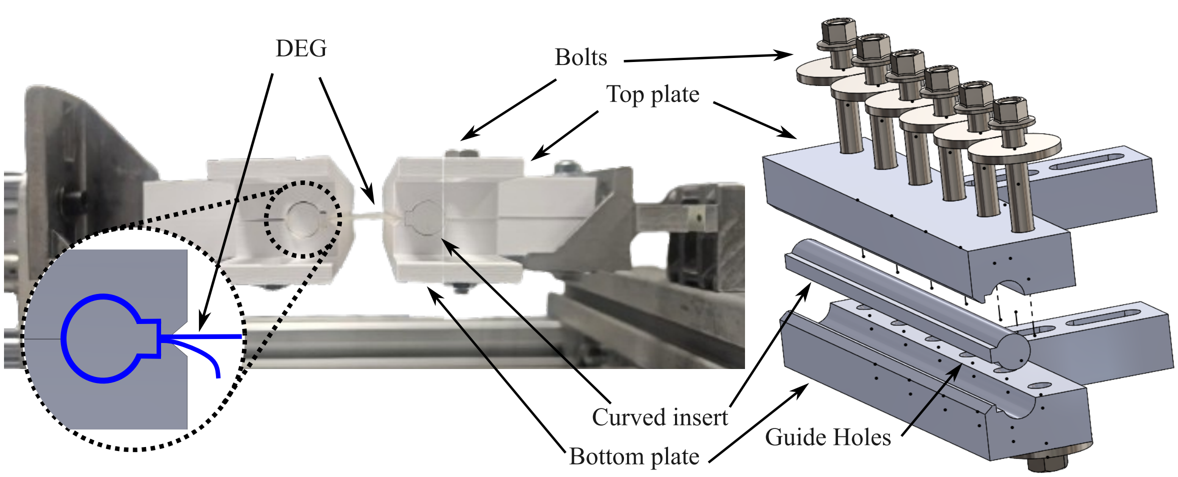

Figure S2: Clamping mechanism for the DEG sample

S2 Observer-like filter for derivative estimation

The observer-like filter described by Eqs. (6-8) allows estimating the derivative of an input signal $y(t)$ by relying on the assumption that the signal has a narrow band around a target frequency $\bar{f} = \bar{\omega}/(2\pi)$. The derivative estimation is always perfect at $f = \bar{f}$, while errors may be introduced at frequencies around

$\bar{f}$. The bandwidth of the filter, i.e., the frequency band around $\bar{f}$ within which the observer consistently estimates the derivative, can be calibrated leveraging the gains $L_1,\ L_2,\ L_3$.

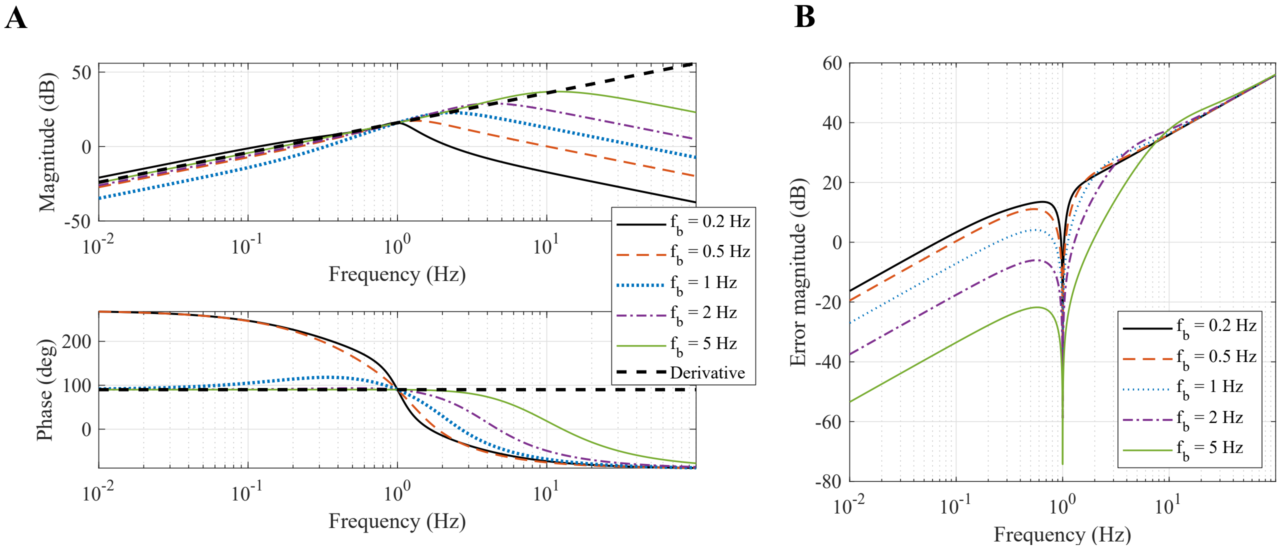

Figure S3: A. Bode plots of the transfer function of different realisations of filter (8) with different target bandwidth. The thick dashed line represents the target transfer function of an ideal derivator; B. Magnitude of the difference (error) between the transfer functions of the different realisations of the filter and the targe ideal derivator.

For the sake of exemplification, in Fig. S3 we report the transfer functions of different realisations of the filter designed with different exponential decay rates α_p and fixed base frequency $\bar{f} = 1$ Hz. Here, the exponential decay rate is defined as the smallest real value $\alpha_p > 0$ such that all the filter eigenvalues have real parts smaller than $-\alpha_p$. Such value formally reflects the convergence time of the system transient response, and can be considered a measure of the bandwidth of the differentiator filter. The parameters for the different implementations were obtained using an automatic design procedure that implements the following optimization problem: select L in such a way that all eigenvalues of (8) have real parts smaller than $-\alpha_p$ with $\alpha_p = 2\pi f_b$ and, at the same, the $\mathcal{H}_2$ norm from y to $\hat{y}$ in (8) is minimized. Such a design problem can be effectively converted in a semidefinite optimization problem using the linear matrix inequalities framework (see Duan & Yu, 978-1-4665-8300-9).

The plots show that it is possible to calibrate the filter and provide an accurate estimate of the derivative in a broad range around the peak frequency. Increasing the bandwidth f_b, however, comes at the cost of an increase in the $\mathcal{H}_2$ norm of the filter (mapping the input signal y into its derivative). In the example of Fig. S3, the squared $\mathcal{H}_2$ norm for $f_b = 5$ Hz is approximately 6000 times larger than that of $f_b = 0.2$ Hz. Since the squared $\mathcal{H}_2$ norm of the transfer function is a measure of the amplification factor of the input signal noise power, increasing the bandwidth indefinitely leads to a magnification of the measurement noise of $y(t)$. Calibration of the filter should thus realise a trade-off between the bandwidth and the resulting noise in the derivative estimation, and it ultimately depends on the quality of the measured signal $y(t)$.

S3 Supplement to the experimental data

The following plots complement the results presented in the main manuscript.
Fig. S4 refers to the same experiments presented in Fig. 3 C-D, showing the instantaneous generated power (positive if power is supplied by the DEG to the circuit).
Fig. S5 presents additional experiments on real-time control with polychromatic excitation, considering

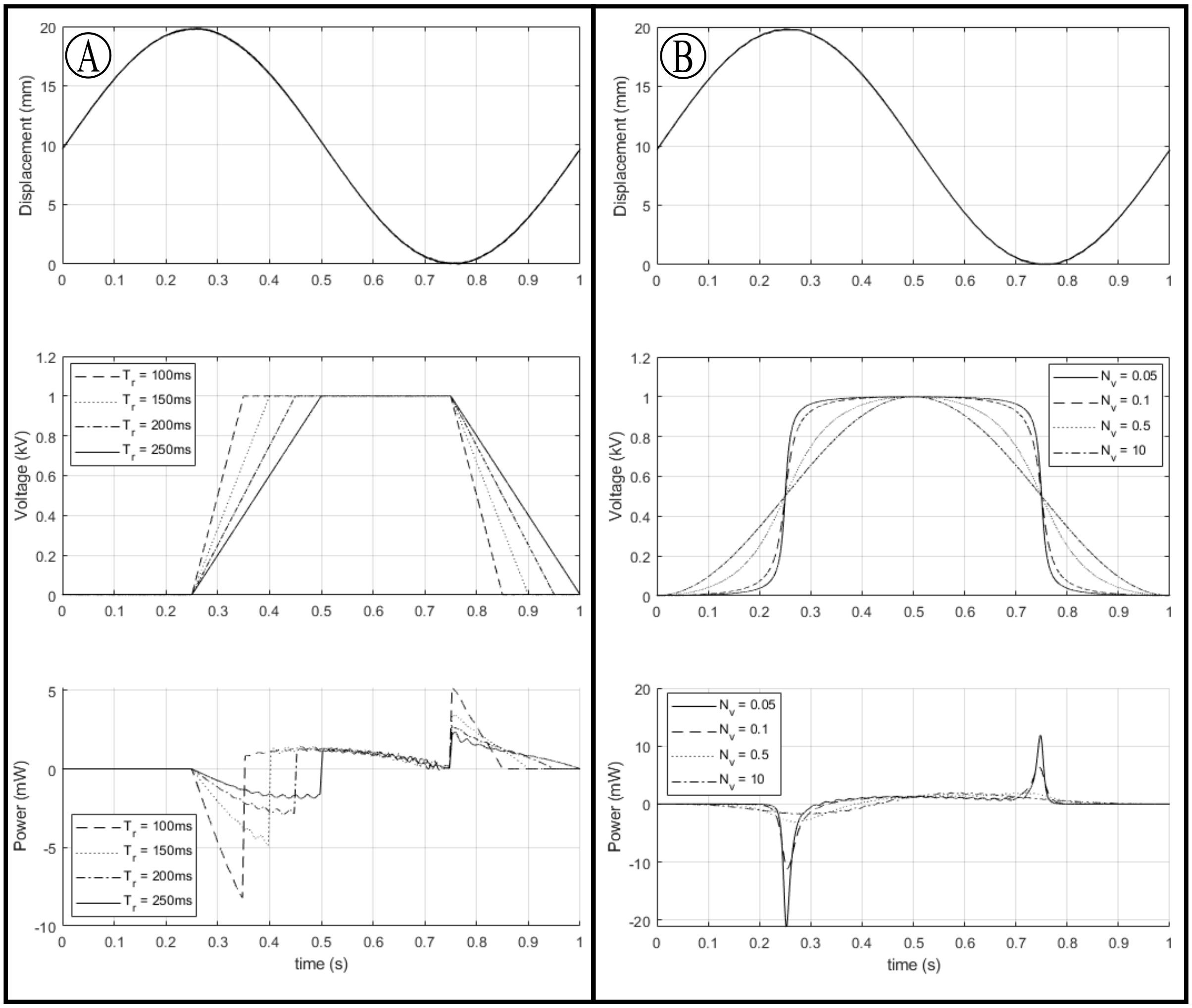

Figure S4: Timeseries of the DEG sample displacement, applied voltage, and instantaneous power output for open-loop peak-triggered (A.) and quadrature (B.) controls, for the tests presented in Fig. 3 in the main manuscript.

different values of the Weibull shape factor κ that describes the excitation signal power spectral density.

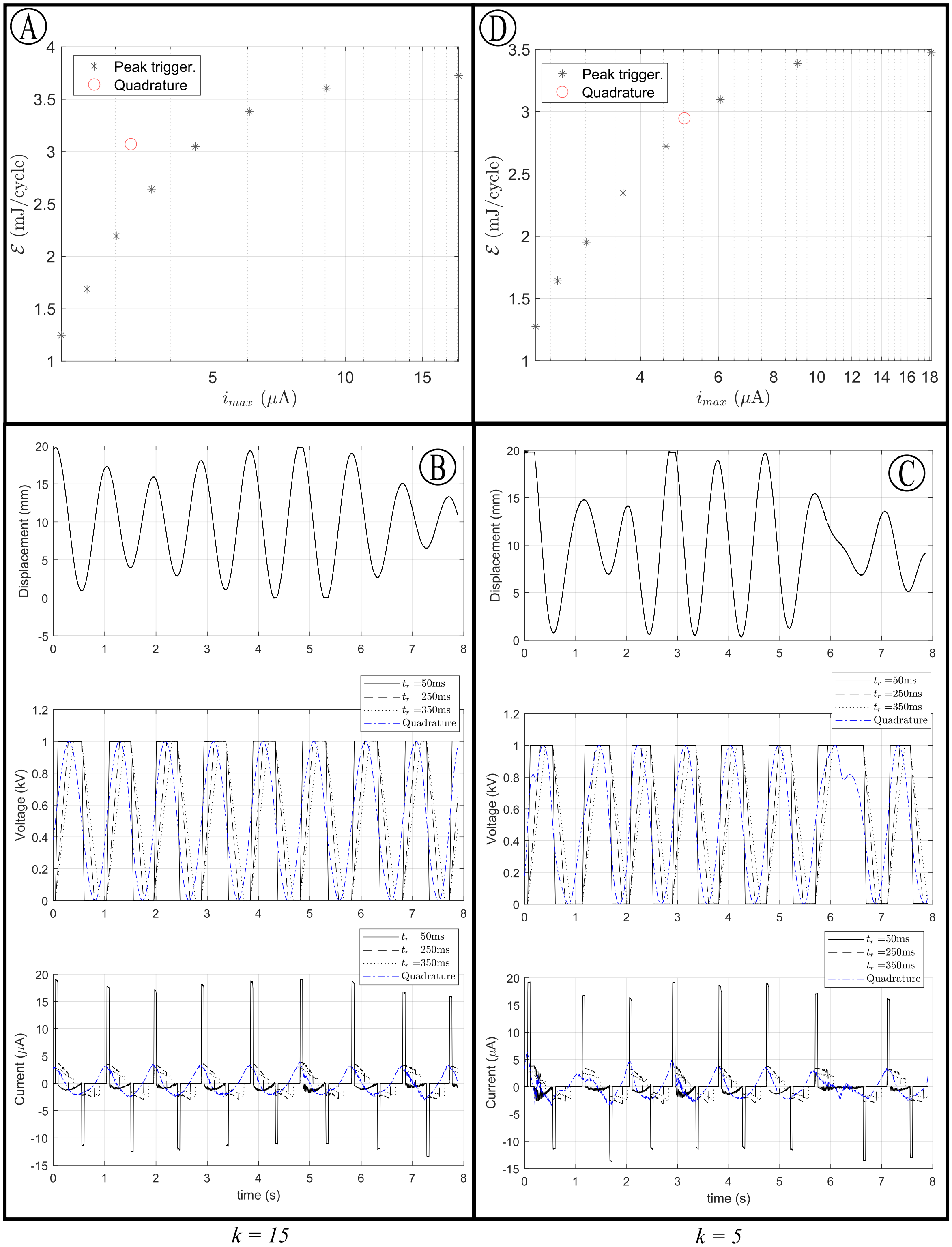

Figure S5: Additional results for real-time control tests with multichromatic excitations with different spectral parameters (Weibull shape factor κ A. Average energy generated per cycle as a function of the peak frequency, and B. time-series of displacement, voltage and current for $\kappa = 15$. C. Average energy generated per cycle as a function of the peak frequency, and D. time-series of displacement, voltage and current for $\kappa = 5$.